Image Reconstruction from 2D stack of MRI/CT to 3D using Shapelets

Arathi T[1], Latha Parameswaran[2]
[1]PhD Scholar, [2]Professor,
Department of Computer Science and Engineering, Amrita Vishwa Vidyapeetham
Ettimadai, Coimbatore, India
[1] arathiviswam09@gmail.com
[2] p_latha@cb.amrita.edu

Abstract—Image reconstruction is an active research field, due to the increasing need for geometric 3D models in movie industry, games, virtual environments and in medical fields. 3D image reconstruction aims to arrive at the 3D model of an object, from its 2D images taken at different viewing angles. Medical images are multimodal, which includes MRI, CT scan image, PET and SPECT images. Of these, MRI and CT scan images of an organ when taken, is available as a stack of 2D images, taken at different angles. This 2D stack of images is used to get a 3D view of the organ of interest, to aid doctors in easier diagnosis. Existing 3D reconstruction techniques are voxel based techniques, which tries to reconstruct the 3D view based on the intensity value stored at each voxel location. These techniques don't make use of the shape/depth information available in the 2D image stack. In this work, a 3D reconstruction technique for MRI/CT 2D image stack, based on Shapelets has been proposed. Here, the shape/depth information available in each 2D image in the image stack is manipulated to get a 3D reconstruction, which gives a more accurate 3D view of the organ of interest. Experimental results exhibit the efficiency of this proposed technique.

Keywords-Image reconstruction, Shapelets, Voxel, Isosurface reconstruction, Marching cubes, Surface to volume reconstruction

I. INTRODUCTION

Different imaging techniques are available to acquire images of the human body. Computerized Tomography scanners allow obtaining the images of dense structures like bones, while Magnetic Resonance Imaging scanners help in the visualization of softer tissues. Positron Emission Tomography (PET) gives information about the blood flow activity inside the human body, while SPECT images allow the analysis of the physiological changes in the body. Of these techniques available, the images obtained after the CT scan or MRI of an organ is available as a stack of 2D images. The CT as well as the MRI scanners rotates 360 degrees to get the image of each slice of the organ of interest. The slice separation and the scanner step in degrees for each image can be adjusted prior to the scanning process, as required by the doctor. A 3D reconstruction of the organ, from this 2D stack of MRI/CT images gives a view of the organ at 360 degrees. This aids doctors to get a clear view of the problems concerning the organ, which is much simpler and more accurate, than having to study all the 2D images from the original stack.

3D image reconstruction has seen extensive research and some algorithms have been developed, as solutions for obtaining a 3D model of an object with multiple 2D views. 3D reconstruction techniques can be widely classified as Active and Passive. Active reconstruction technique includes shape from optical triangulation [1], where 2D images of the object is taken, by turning it 360 degrees. From each 2D image thus obtained, sample points are taken, which are then used to form triangles, to finally arrive at its shape. This technique is commonly known as shape from stereo reconstruction [2]. The passive techniques include techniques like, shape from silhouette [3], shape from shading [4], voronoi based reconstruction [5], reconstruction from point clouds [6] and reconstruction from unorganized points [7].

All the 3D reconstruction techniques existing till date aims to decrease the processing time [8], reduce the storage space [9] and to increase the accuracy. An accurate 3D reconstruction was conventionally achieved in these techniques, by selecting different ways to develop an efficient mesh structure of the object, rather than manipulating the depth information from the dataset. Most of the existing 3D reconstruction techniques for MRI/CT are voxel based techniques, which tries to reconstruct the 3D view based on the intensity value stored at each voxel location. The voxel based techniques available for 3D reconstruction of MRI/CT images are Marching cubes algorithm [10], Isosurface reconstruction [11] and surface to volume reconstruction [12]. These techniques do not make use of the shape/depth information available in the 2D image stack. In this paper, a 3D reconstruction technique for MRI/CT is developed, using Shapelets [13, 14]. Wavelets [15] decompose an image on several scales, but fail to describe the real shape of an object. Shapelets do not decompose an image on different scales, but on different elementary shapes. This enables shapelets to capture the shape information in the image. Hence, it can be used to extract the shape information in an image, which in turn is hidden in the

depth information. The proposed technique gets the depth information from each slice in the 2D stack of MRI/CT image and generates the shape for each image slice. Experimental results show that the proposed technique provides a more accurate 3D representation of the organ, than the voxel based reconstruction techniques.

II. SHAPELETS

Wavelet decomposition allows decomposing an image on several scales. But they fail to describe the real shape of an object. Shapelets decompose an image based on different elementary shapes. Shapelet decomposition is a linear decomposition of an image into a series of localized basis functions with different shapes. Shapelets are of two types namely Cartesian shapelets and Polar shapelets.

A. Cartesian Shapelets

They are weighted Hermite polynomials, which correspond to perturbations about a circular Gaussian [14]. The dimensionless basis function is defined as:

$$\phi_n(x) = \left[2^n \sqrt{\pi} n!\right]^{-1/2} H_n(x) e^{-x/2}$$

$\boldsymbol{H_n}$ is an n^{th} order Hermite polynomial. They are orthogonal. i.e.

$$\int_{-\infty}^{\infty} dx \phi_n(x) \phi_m(x) = \delta_{mn}$$

For practical applications, the dimensional basis function is used:

$$B_n(x;\beta) \equiv \beta^{-1/2} \varphi_n\left(\frac{x}{\beta}\right)$$

β is a character size, close to that of the object which is to be decomposed. The basis functions B_n are also orthogonal. The object to be decomposed is thus represented as:

$$f(x) = \sum_{n=0}^{\infty} f_n B_n(x;\beta)$$

The shapelet coefficient is given by:

$$f = \int_{-\infty}^{\infty} dx f(x) B_n(x;\beta)$$

If the object is adequately localized, the series converges quickly, so that the first few basis functions are sufficient to approximate the shape information of the object of interest. Then, its decomposition into shapelets can be truncated to some maximum order of decomposition.

$$f(x) = \sum_{n=0}^{n_{\max}} f_n B_n(x;\beta)$$

Figure 1 shows 1D and 2D Cartesian shapelets.

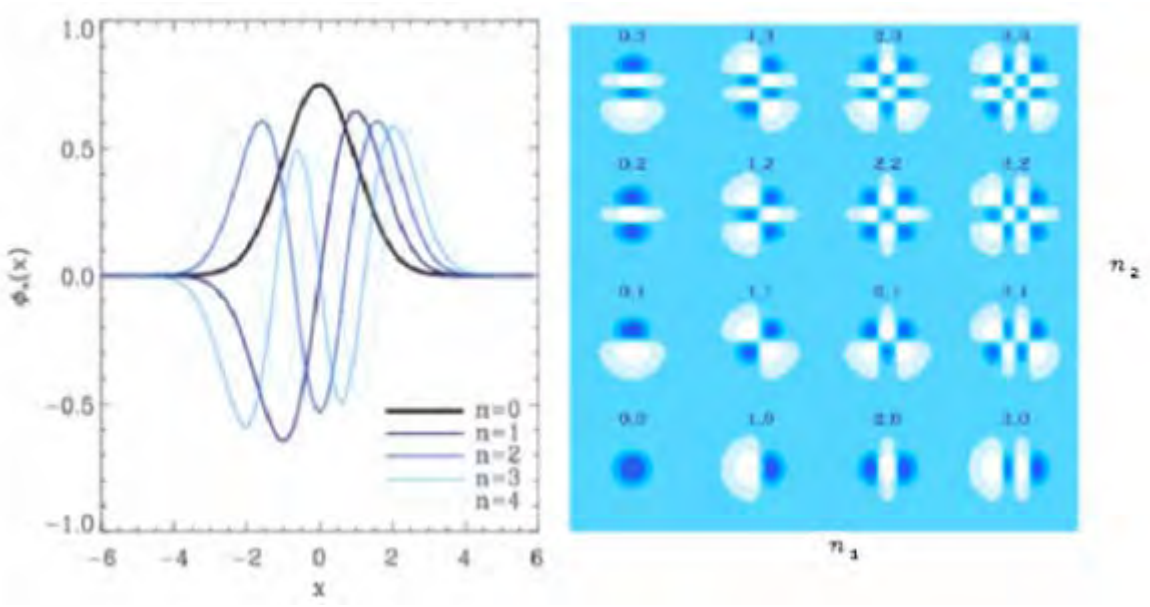

Fig. 1. Cartesian Shapelets

B. Polar Shapelets

They are similar to Cartesian shapelets, with a Gaussian weighting function of scale size β. Since they are polar, they are separable in 'θ' and 'r' and hence easier to understand. Also, the operations on them are more intuitive.

A function $f(r,\theta)$ in polar coordinates can be decomposed as a weighted sum of the basis functions $\chi_{n,m}(r,\theta;\beta)$:

$$f(r,\theta)=\sum_{n=0}^{\infty}\sum_{m=-n}^{n} f_{n,m}\chi_{n,m}(r,\theta;\beta)$$

$$f_{n,m}=\int\int_{R} f(r,\theta)\chi_{n,m}(r,\theta;\beta)rdrd\theta$$

$f_{n,m}$ ($n \varepsilon N$, $-n \leq m \leq n$) are the polar shapelet coefficients of order (n, m). The real and imaginary parts of the first few polar shapelets are given in Figure 2.

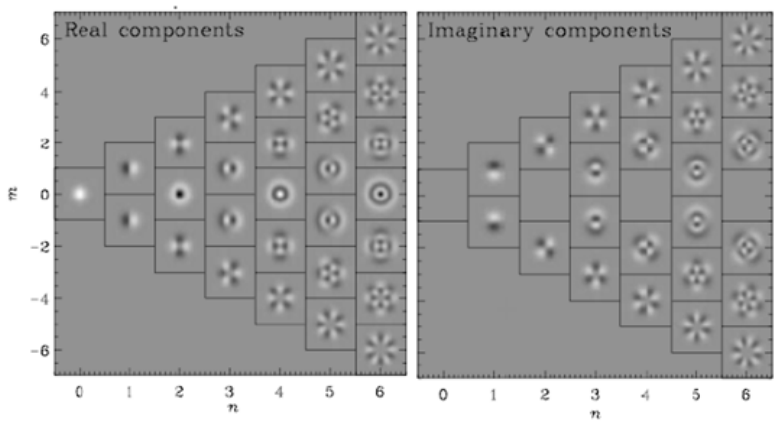

Fig. 2. First few polar shapelet basis functions $\chi_{n,m}$

C. Constructing the surface normals

Traditionally, surfaces where reconstructed from surface normals via integration. However, to do this, the surface gradients should be integrable. This approach is also sensitive to noise.

Since differentiation is linear, a correlation performed between the signal gradient and the gradients of the basis function provide information, is proportional to the direct correlation between the signal and the basis function. Hence, if the surface gradient information is correlated with the gradients of a bank of shapelet basis functions, the surface shape can be reconstructed by summing the results of correlation. The summing of the

correlated values of the basis automatically imposes a continuity constraint and performs an implicit integration of the surface from its gradients [14].

Correlation between the gradients of the surface and each shapelet is defined in terms of slant and tilt values separately and then combined. The correlation of the surface and the shapelet slants is done in terms of the gradient magnitude, which is given by the tan of the slant.

$$|\nabla| = \tan(\sigma)$$

The gradient correlation is then formed as:

$$C_{\nabla} = \sum_{x}\sum_{y} |\nabla_f \| \nabla_s|$$

f – denotes the surface and *s* denotes the shapelet.

Tilt values are used to make a distinction between positive and negative shapes in the image. If the surface and shapelet gradient magnitudes match at some point, and the tilt directions also match, then the component of the shapelet at this point must be positive. If the tilts of the surface and the shapelet are in opposite directions, then the shapelet component must be negative. If the tilts are orthogonal, then there is no correlation between the surface and the shapelet. Thus, the gradient correlation must be multiplied by a tilt correlation measure, which varies between 1 and -1, when the tilts are in opposite directions. A measure that satisfies this requirement is the cosine of the tilt angle difference.

$$\begin{aligned} C_{\tau} &= \sum_{x}\sum_{y} \cos(\tau_f - \tau_s) \\ &= \sum_{x}\sum_{y} \cos(\tau_f)\cos(\tau_s) + \sum_{x}\sum_{y} \sin(\tau_f)\sin(\tau_s) \end{aligned}$$

The overall correlation measure between the surface and the shapelet is obtained by the product of the gradient and the tilt correlations:

$$\begin{aligned} C &= C_{\nabla} C_{\tau} \\ &= \sum_{x}\sum_{y} |\nabla_f \| \nabla_s| \left[\sum_{x}\sum_{y} \cos(\tau_f)\cos(\tau_s) + \sum_{x}\sum_{y} \sin(\tau_f)\sin(\tau_s) \right] \\ &= \sum_{x}\sum_{y} |\nabla_f| \cos(\tau_f) . |\nabla_s| \cos(\tau_s) + \sum_{x}\sum_{y} |\nabla_f| \sin(\tau_f) . |\nabla_s| \sin(\tau_s) \end{aligned}$$

The '.' denotes point-wise multiplication. This is performed over multiple scales of the shapelet and the result is summed to form the final reconstruction.

$$R = \sum_{i} C_i$$

D. Choosing the shapelet basis

A large number of basis functions are available that can be used as shapelets. Correlating the gradient of one shapelet filter with the gradient of the signal corresponds to extracting a band of frequencies from the signal gradient. The need to reconstruct a surface from correlations between surface normals and shapelet gradients imposes the following constraints on the shapelet function:

- Minimal ambiguity of shape with respect to its gradient.
- Preservation of phase information in the signal.
- Uniform coverage of the signal spectrum, so that it is faithfully reconstructed.

The commonly used shapelet for image decomposition is the 2D Cosine Gabor wavelet. Figure 3 shows its smoothly varying normals. But the gradient magnitudes have discontinuities of slope.

Fig. 3. Cosine Gabor function (left), its gradient magnitude (right)

Figure 4 shows a shapelet based on low-pass Butterworth filter.

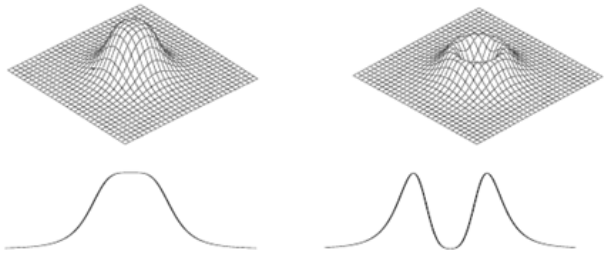

Fig. 4. Butterworth shapelet with transition parameter n=2, along with its cross-section (left), its gradient magnitude (right)

In order to select a shapelet with minimal ambiguity of shape with respect to its gradient, it must be simple and ideally take the form of a single peak, so that the gradient function will have a single positive and a single negative peak. A function which satisfies this criterion is the Gaussian filter. Hence, for the experiments presented in this work, the shapelet used is the Gaussian shapelet. Figure 5 shows the Gaussian shapelet.

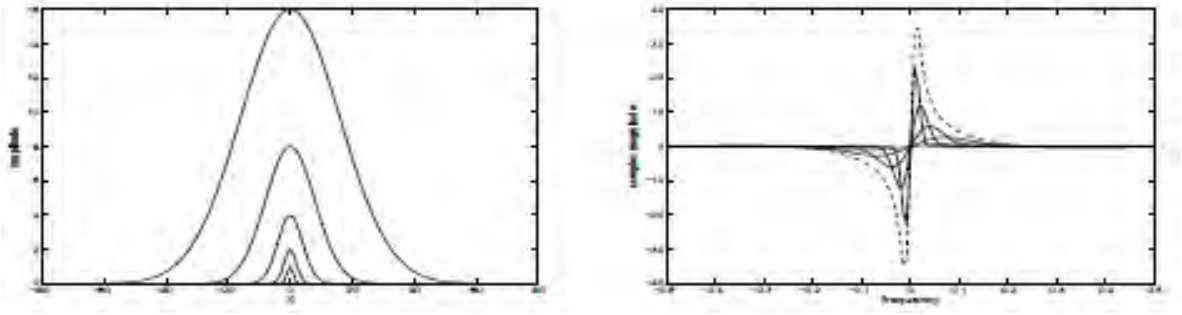

Fig. 5. A shapelet bank of 5 Gaussians, with height proportional to scale (left), The corresponding transfer functions of their gradients (right). The sum of the transfer functions is shown by the dashed line.

III.PROPOSED RECONSTRUCTION ALGORITHM

3D reconstruction aims at generating an accurate 3D model of the organ of interest, with minimal ambiguity. At the same time, it should preserve all the information in each slice of the 2D image stack. The reconstruction technique presented here ensures that the above requirements are met. The highlight of this technique is in the fact that, it makes use of the shape/depth information, which is hidden in the 2D stack and manipulates it to generate the 3D view. This ensures a greater accuracy in the final generated 3D view.

The input to the method is a 2D stack of *'N'* MRI/CT images. Each image in the stack is called a slice. The following are the steps carried out on each of the slices S_i, $i = 1, 2….N$, in order to generate the final 3D view.

A. Generating the gradient values in the two directions

Each slice S_i is taken and the gradients in the ***x*** and ***y*** directions are obtained respectively as S_{dx} and S_{dy}.

B. Obtaining the Slant and Tilt values for each slice

The gradients thus obtained are used to get the slant and tilt values.

C. Finding the gradient correlation

The gradient correlation measure is obtained by multiplying and summing the gradient magnitudes of the surface $\left|\nabla_f\right|$ and that of the shapelet $\left|\nabla_s\right|$.

$$C_{\nabla} = \sum_x \sum_y \left|\nabla_f\right| \left|\nabla_s\right|$$

D. Getting the tilt correlation

The tilt correlation measure is generated using the expression:

$$C_{\tau} = \sum_x \sum_y \cos\left(\tau_f - \tau_s\right)$$

E. Obtaining the overall correlation between the surface and the shapelet

The gradient and tilt correlation measures are multiplied to obtain the overall correlation measure.

$$C = C_{\nabla} C_{\tau}$$

F. Getting the final reconstruction

This process is carried out on different scales of the shapelets and the correlation measures thus obtained for each case is then summed up to get the final reconstruction.

$$R = \sum_{i} C_i$$

G. Generating the final 3D view

The above steps are repeated on each of the image slice in the 2D stack and the summed up correlations for each slice is finally stored together to build a volume. This volume is then rendered using rendering techniques like isosurface reconstruction and surface to volume reconstruction.

IV. EXPERIMENTAL RESULTS

The proposed 3D reconstruction technique has been evaluated on a number of sets of 2D stack of MRI/CT images. The results pertaining to three sets are shown here. Set 1 is a stack of CT image of the head, with 40 2D grayscale images. Set 2 is a stack of CT image of the head with 99 2D grayscale images. Set 3 is a stack of MRI image of the head, with 99 2D grayscale images. Each 2D image in the stack for all the 3 sets is having a size of 256 x 256.

The proposed technique has been applied to these 3 sets of images. To compare the accuracy of the generated 3D model, the 3D reconstruction of the same set of images has also been carried out using voxel based rendering techniques.

a) 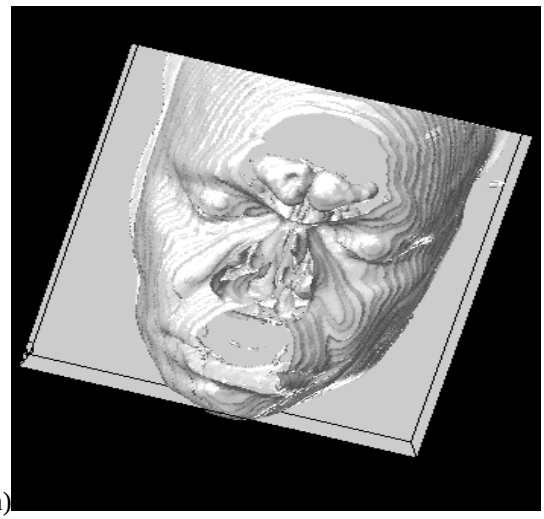

b) 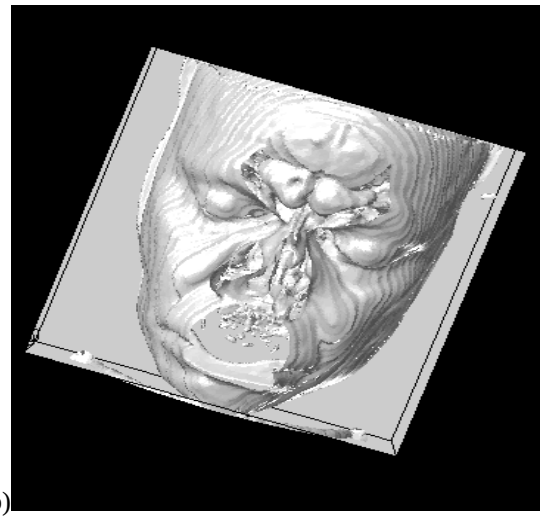

c) 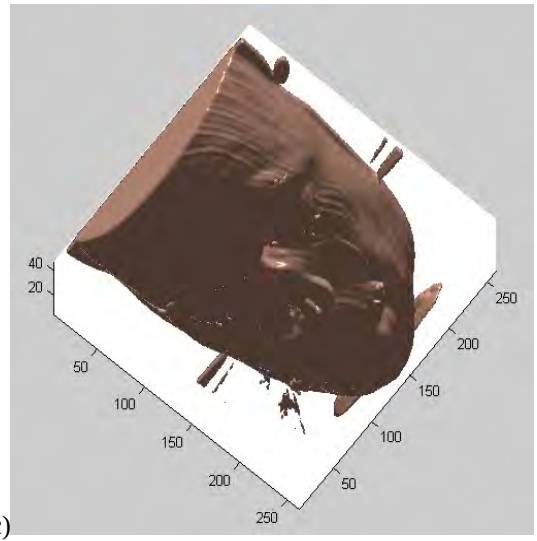

e) 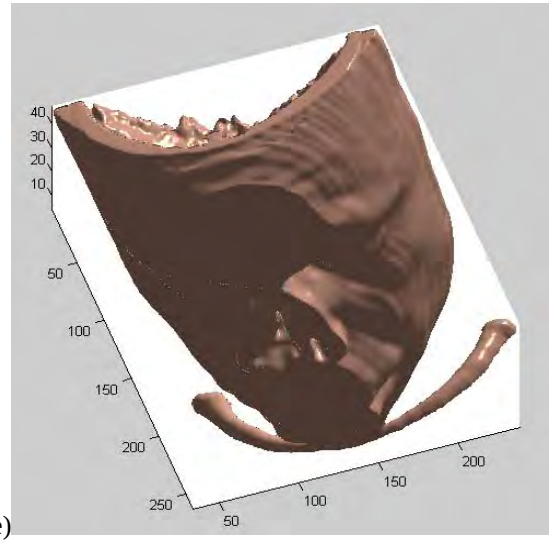

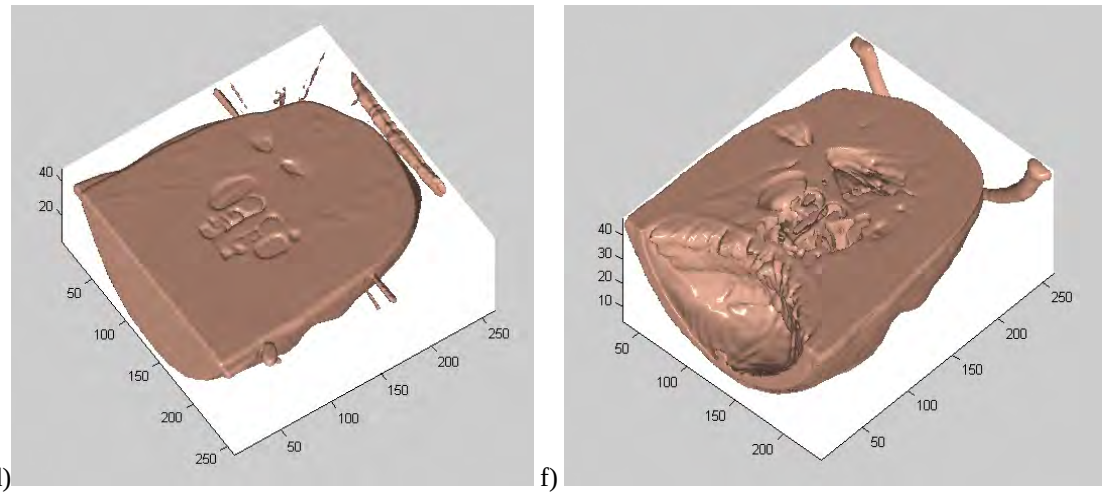

Fig. 6. SET 1 - a) Voxel based isosurface rendering, b) Shapelet based isosurface rendering, Voxel based surface to volume rendering c) Front view d) Back view, Shapelet based surface to volume rendering e) Front view f) Back view

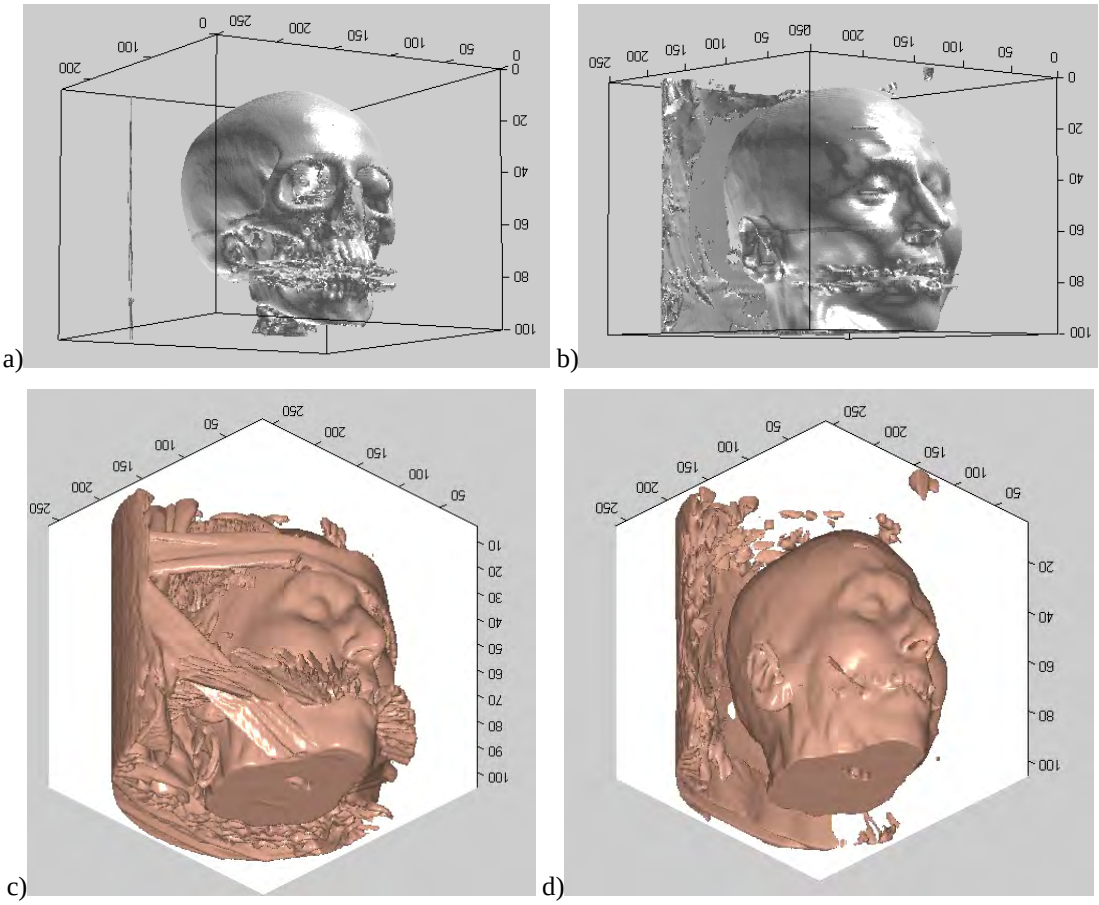

Fig. 7. SET 2 - a) Voxel based isosurface rendering, b) Shapelet based isosurface rendering, c) Voxel based surface to volume rendering, d) Shapelet based surface to volume rendering

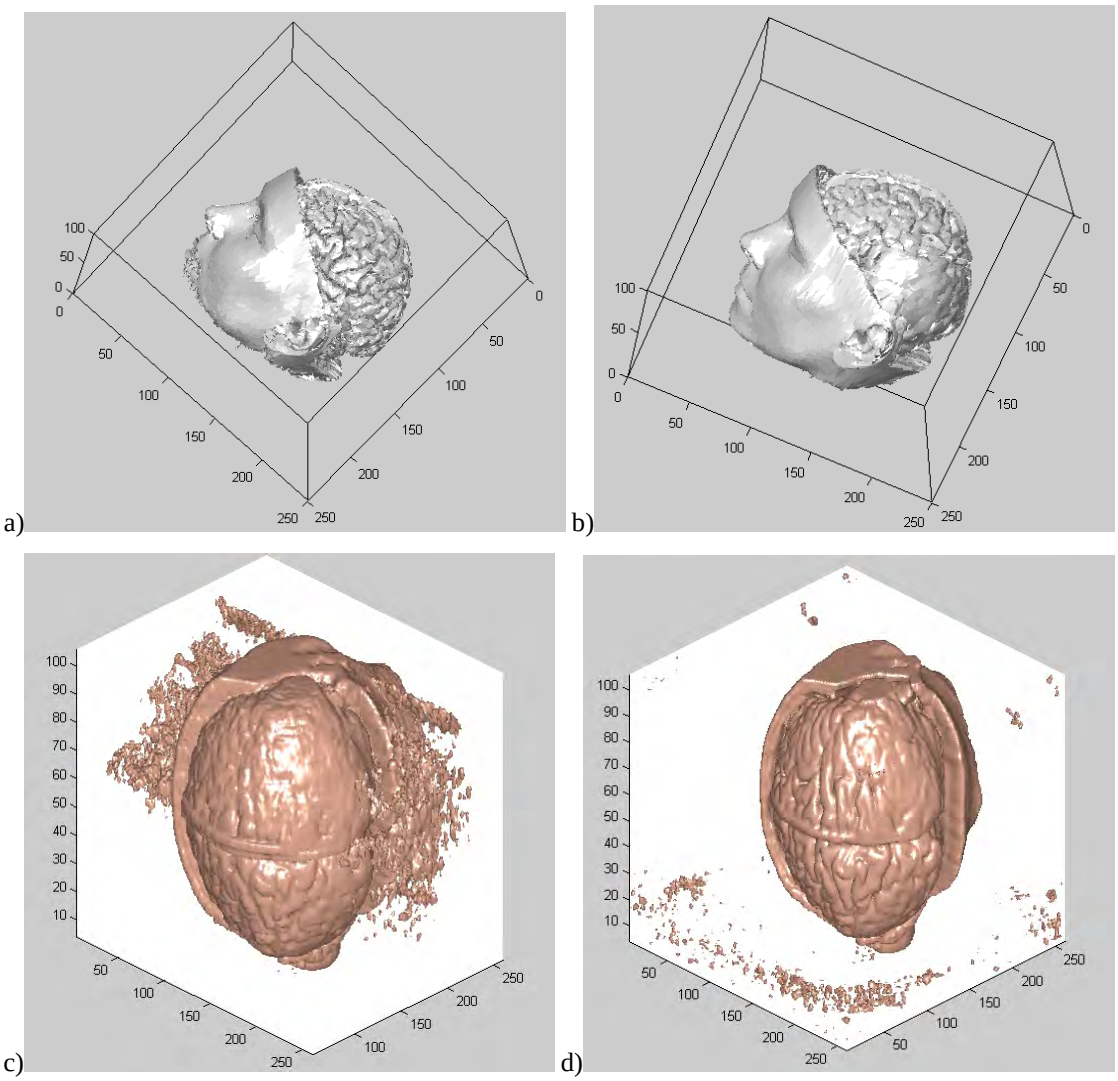

Fig. 8. SET 3 - a) Voxel based isosurface rendering, b) Shapelet based isosurface rendering, c) Voxel based surface to volume rendering, d) Shapelet based surface to volume rendering

The result obtained from two rendering techniques has been shown for each set of images. The isosurface rendering technique gives a view of the structure of the organ, while the surface to volume rendering creates a smooth surface of the organ. The former is used by doctors to get a detailed knowledge of the organ under study, while the latter assists doctors in plastic surgery, cosmetic surgeries like maxillofacial surgery, craniofacial surgery, microvascular reconstruction to study head and neck cancer etc.

From the results, it is clearly evident that the proposed shapelet based 3D reconstruction method gives a more accurate 3D view of the concerned organ, than its voxel based 3D view. It can be seen that the small details about the organ is clearly visible in the 3D view, when the proposed technique is used. These minute details are missing in the conventional voxel based techniques. Also, the surfaces obtained by the proposed method is smoother and better resembles the organ, than the conventional techniques. This is because; the proposed method extracts the complete shape information from the input stack and then constructs a 3D model.

V. CONCLUSION

Conventional 3D reconstruction techniques for MRI/CT images try to develop an efficient mesh structure, followed by a voxel based rendering of the stored data. It fails to utilize the shape/depth information which is available in the acquired medical images. Shapelets overshadows wavelets in their capability to accurately represent the shape of an object. Shapelets are used to obtain the gradient information from each image in the 2D MRICT image stack. This in turn is used to get the depth information. The correlation between the shapelet and the image slices are stored in a volume and then rendered using isosurface reconstruction and surface to volume reconstruction. Experiments were conducted on steps of MRI/CT image stacks. 3D reconstruction was also carried out using voxel based rendering techniques. The results demonstrate that the proposed method gives a noticeably better 3D representation of the organ, than the conventional techniques.

REFERENCES

[1] F. Cazals, J. Giesen, "Delaunay triangulation based surface reconstruction", Springer- Verlag, Mathematics and Visualization, pp. 231–276, 2006.

[2] H. Hirschmueller, "Stereo Processing by Semiglobal Matching and Mutual Information", IEEE Transactions on Pattern Analysis and Machine Intelligence, Vol. 30, No. 2, pp. 328-341, February 2008.

[3] Y. Temez, C.J Wetherilt, "A volumetric fusion technique for surface reconstruction from silhouettes and range data", Journal of Computer Vision and Image Understanding, Elsevier, pp. 30-41, 2007.

[4] C.N Carter, R.J Pusateri, Dongqing Chen, A.H. Ahmed, A.A Farag, " Shape from shading for hybrid surfaces as applied to tooth reconstruction", 17th IEEE International Conference on Image proceesing, 26-29 September, 2010.

[5] P Alliez, D. Cohen-Steiner, Y.Tong, M.Desbrun, " Voronoi-based Variational Reconstruction of Unoriented Point Sets", Eurographics Symposium on Geometry Processing, 2007.

[6] Boris Mederos, Nina Amenta, Luiz Velho, Luiz Henrique de Figueiredo, "Surface reconstruction from Noisy Point Clouds", Eurographics Symposium on Geometry Processing, 2005.

[7] Marek Vanco, Bernd Hamann, Guido Brunnett, "Surface reconstruction from Unorganized Point data with Quadrics", Computer graphics forum, pp 1-15, 2007.

[8] Qianqian Fang, David A. Boas, "Tetrahedral Mesh generation from volumetric Binary and Garyscale Images", International Symposium on Biomedical Imaging of IEEE, 2009.

[9] Bernard Finkbeiner, Alireza Entezari, Torsten Moller, "Efficient Volume Rendering on the Body Centered Cubic Lattice using Box Splines", SFU School of Computing, Technical Report, 2009.

[10] W. Lorensen, H. Cline, "Marching Cubes: A High Resolution 3D Surface Construction Algorithm", ACM Computer Graphics, Volume 21, No: 4, July 1987.

[11] B. Mora, J.P Jessel, R. Caubet, "Visualization of Isosurface with Parametric Cubes", Eurographics publications, volume 20, No: 3, 2001.

[12] H. Hauser, L.Mroz, G. Italo Bischi, E Groller, "Two-level Volume Rendering", IEEE Transactions on Visualization and Computer Graphics, Volume 7, No: 3, pp: 242-252, 2001.

[13] Joel Berge, Richard Massey, Aleandre Refregier, "An introduction to shapelets based weak lensing image processing", Shapelets package version 2.2, manual for users, 2006.

[14] B. Karacali, W. Snyder, "Partial integrability in surface reconstruction from a given gradient field", IEEE International Conference on Image Processing, Volume 2, pp: 525–528, 2002.

[15] S.G. Mallat, "A Wavelet Tour of Signal Processing", Academic press, 1999.

AUTHOR PROFILE

Arathi T has a B.Tech degree in Electronics and Communication Engineering and a M.Tech degree in Remote Sensing and Wireless Sensor Networks from Amrita Vishwa Vidyapeetham, Coimbatore. She is currently pursuing her PhD from Amrita Vishwa Vidyapeetham, Coimbatore. She has 5 years experience in teaching and 4 years in research. She is currently working as Assistant Professor in the Department of Electronics and Communication Engineering, LBS College of Engineering, Kasaragod, Kerala. Her research interests are Image processing, Signal processing, Wavelets and Support Vector Machines.

Latha Parameswaran has a Bachelor's degree in Mathematics and a Master's degree in Computer Applications from Bharathiar University and a Ph.D from Bharathiar University. She has 10 years experience in IT industry and 13 years experience in teaching and research. She is currently a Professor at the Department of Computer Science and Engineering, Amrita Vishwa Vidyapeetham, Coimbatore. Her research interests are digital image processing and analysis, information security, data mining and theoretical computer science.